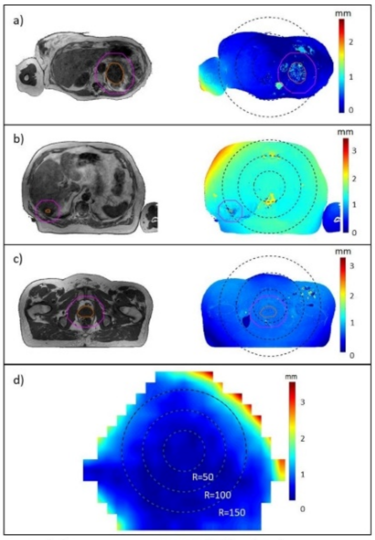

Fig. 1: a)-c) Representative T2W MRI (left) and B_0 distortion maps (right). Red ROI denotes the GTV, and magenta ROI shows a 30 mm region around the GTV. Black dotted lines show concentric circles centered at iso-center and with radii of 50, 100 and 150 mm, respectively, to indicate the additional level of distortion from gradient non-linearity of the 1.5 T MR-Linac (d) . a) Adrenal gland (pt. 3). b) Liver metastasis (pt. 1). c) Prostate (pt. 2).

Table 1: Extracted distortions related to B_0 and gradient non-linearity (GNL) for individual patients.

Clinical 3D T2W		GTV [mm]			30 mm around GTV [mm]			Est. GNL contribution [mm]
		Mean	Median	Std. dev.	Mean	Median	Std. dev.	Range
Adrenal gland	1	0.17	0.15	0.18	0.14	0.12	0.13	0 - 1
	2	1.92	1.71	0.51	1.64	1.63	0.28	0 - 1
	3	0.38	0.20	0.36	0.23	0.17	0.25	0 - 1
	4	1.38	1.34	0.15	1.37	1.35	0.14	0 - 1
	5	1.07	0.80	0.67	0.82	0.75	0.39	0 – 1
	6	0.56	0.56	0.07	0.62	0.61	0.14	0 – 1
	7	1.56	1.63	0.25	1.62	0.56	0.30	0.5 - 2
	Mean	1.01 ± 0.65	0.91 ± 0.65	-	0.92 ± 0.63	0.74 ± 0.56	-	-
Liver	1	1.19	1.21	0.12	1.26	1.28	0.17	0.5 – 1.5
	2	0.69	0.66	0.09	0.70	0.68	0.10	0.5 – 2.5
	3	1.55	1.54	0.14	1.41	1.43	0.17	0 - 1
	Mean	1.14 ± 0.44	1.14 ± 0.45	-	1.12 ± 0.37	1.13 ± 0.40	-	-
Prostate	1	0.85	0.82	0.10	0.90	0.80	0.32	0 - 1
	2	0.78	0.80	0.13	0.79	0.80	0.12	0 - 1
	3	0.50	0.79	0.40	0.75	0.82	0.24	0 - 1
	4	1.36	1.68	0.43	1.23	0.94	0.50	0 - 1
	5	0.12	0.12	0.05	0.13	0.13	0.06	0 - 1
	6	0.10	0.09	0.10	0.13	0.10	0.12	0 - 1
	7	0.06	0.03	0.14	0.06	0.04	0.13	0 - 1
	8	0.91	0.91	0.07	0.91	0.88	0.17	0 - 1
	9	0.77	0.77	0.22	0.76	0.76	0.10	0 - 1
	10	0.65	0.67	0.10	0.63	0.65	0.12	0 - 1
	11	0.85	0.86	0.12	0.84	0.84	0.11	0 - 1
	12	0.13	0.09	0.18	0.11	0.10	0.11	0 - 1
	13	1.86	1.73	0.37	1.69	1.69	0.24	0 - 1
	14	0.77	0.78	0.11	0.77	0.77	0.10	0 - 1
	15	0.79	0.79	0.09	0.78	0.78	0.08	0 - 1
	Mean	0.87 ± 0.36	1.02 ± 0.44	-	0.92 ± 0.22	0.84 ± 0.07	-	-

Conclusion

The total geometric distortion is tumour site specific (scale with distance to iso-center) and can potentially reach clinically relevant levels in some pts. Ideally, the total distortion should be accounted for in a daily MRI-guided adaptive workflow, which particularly has the aim of delivering treatment with high geometric precision.

PH-0408 Assessment of the generalizability to pediatric protontherapy of a 3D network generating pseudo-CT

E. Alvarez Andres[1,2,3], M. Caussé[2,3], L. Fidon[1], L. Ermeneux[2,4], S. Bolle[5], V. Martin[5], N. Paragios[1], E. Deutsch[3,5], L. De Marzi[6,7], C. Robert[2,3]
[1]TheraPanacea, Radiotherapy, Paris, France ; [2]Department of Medical Physics, Gustave Roussy - Paris-Saclay University, Villejuif, France ; [3]U1030 Molecular Radiotherapy, Paris-Sud University - Gustave Roussy - Inserm - Paris-Saclay University, Villejuif, France ; [4]U1018 Radiation Epidemiology, Paris-Sud University - Gustave Roussy - Inserm - Paris-Saclay University, Villejuif, France ; [5]Department of Radiotherapy, Gustave Roussy - Paris-Saclay University, Villejuif, France ; [6]Centre de protonthérapie d'Orsay, Institut Curie - PSL Research University, Orsay, France ; [7]U1021 Normal and Pathological Signaling: from the embryo to the innovative therapy of cancers, Institut Curie - Inserm - CNRS UMR 3347 - PSL Research University - Paris-Saclay University, Orsay, France

Purpose or Objective

A 3D convolutional neural network was used to map a Magnetic Resonance Imaging (MRI) into a pseudo Computed Tomography (pCT). It was trained and validated on an adults' cohort and tested on a cohort including protontherapy-treated pediatric patients only to evaluate the network robustness.

Material and Methods

The total cohort was composed of 341 brain tumor patients leading to 162 pairs of CT/T1 weighted MRI (T1) and 179 pairs of CT/contrast-enhanced T1 weighted MRI (T1-Gd) pairs. 242 (121 T1–121 T1-Gd) and 81 (41 T1–40 T1-Gd) adult patients were respectively used to train and validate a modified version of the 3D HighResNet (Li et al., 2017). Its main particularities were the residual connections and the dilated convolution filters, ensuring an absence of vanishing/exploding gradient effects and a high network receptive field respectively (Figure 1).

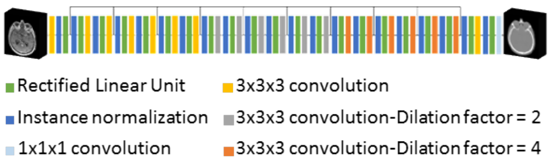

Fig. 1. Architecture of the modified HighResNet.

Generalizability of the network was tested with 18 (18 T1-Gd) pediatric patients with a mean age of 12.5 years treated for a craniopharyngioma with a double scattering protontherapy. The CT plan was transferred to the pCT before recalculating the dose with the pencil beam algorithm implemented in ISOgray 4.2.1 (DOSIsoft). Mean Absolute Error (MAE) within four areas (whole head, air, bone and water), global 1%/1mm, 2%/2mm and 3%/3mm gamma indexes and Dose Volume Histograms (DVH) differences corresponding to the planning target volume were computed to compare CT and pCT image intensities and dosimetric differences.

Results

The computation time for pCT generation was 83s on a single GPU GeForce GTX 1080Ti. Qualitative results are presented in Figure 2.

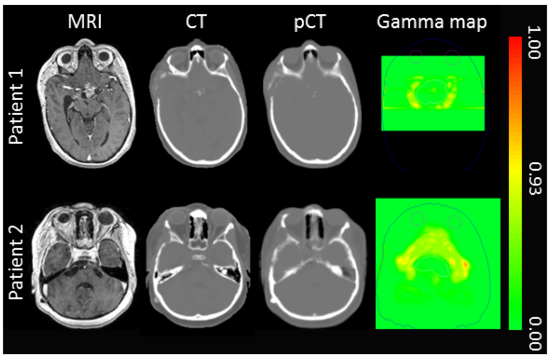

Fig. 2. T1-Gd MRI, CT, pCT and gamma map for the 3%/3mm criterion presented for Patient 1 (17 years old, 6 beams-based treatment) and Patient 2 (6 years old, 6 beams-based treatment). To improve visibility, outer and eyes contours are displayed on the gamma maps.

Mean MAE of 111 Hounsfield Units (HU)+/-12HU, 364HU+/-56HU, 279HU+/-27HU and 60HU+/-10HU were obtained for the whole head, air, bone and water areas respectively. Regarding the dosimetry results, the 1%/1mm, 2%/2mm and 3%/3mm gamma indexes were equal to 96.44%+/-2.22%, 97.92%+/-1.54% and 99.59%+/-0.59% respectively. All 2%, 50%, 95% and 98% mean DVH differences were below 0.3%.

Conclusion

To our knowledge, it is the first study evaluating a 3D network with an unseen patient's category. In a previous study, a test with a cohort composed of 79 adults treated with intensity modulated radiation therapy led to a head MAE of 83HU+/-22HU, and gamma indexes of 97.90%+/-1.10%, 99.61%+/-0.30% and 99.83%+/-0.19% for the 1%/1mm, 2%/2mm and 3%/3mm criteria. As a result, very little differences were observed between the two studies highlighting the high generalizability of the developed model and its clinical implementation feasibility.

PH-0409 Development of materials with independently adjustable MR- and CT-contrast to validate pseudo CTs

A. Elter[1,2,3], P. Mann[1,3], S. Dorsch[1,2,3], A. Runz[1,3], S. Martin[4], C.P. Karger[1,3]

[1]German Cancer Research Center DKFZ, Medical Physics in Radiation Oncology, Heidelberg, Germany ; [2]Heidelberg University, Faculty of Physics and Astronomy, Heidelberg, Germany ; [3]Heidelberg Institute for Radiation Oncology HIRO, National Center for Radiation Research in Oncology NCRO, Heidelberg, Germany ; [4]German Cancer Research Center DKFZ, Department of Radiopharmaceutical Chemistry, Heidelberg, Germany

Purpose or Objective

MR-guidance in radiotherapy has the main advantage of providing a better soft tissue contrast as compared to conventional kV imaging. However, the image quality in MRI is based on more than 40 individually adjustable sequence parameters. To optimize these parameters for the use in radiotherapy, dedicated phantoms capable of representing anthropomorphic MR contrast are essential. Furthermore, a correct representation of CT values is important to create ground truth images for the validation of algorithms to generate pseudo-CTs from MR-images, which are used for dose calculation. In this work, a method to produce phantom materials with individually adjustable T_1 and T_2 relaxation times in MRI was extended to adjust additionally given CT values in the soft tissue range. The dependence of the relaxation times on the modified CT value as well as on the magnetic field strength (0.35T and 1.5T) was investigated.

Material and Methods

Ni-DTPA doped agarose gels were used to create MRI contrast materials with individually adjustable T_1 and T_2 times [1]:

$$\frac{1}{T_{1/2}} = \frac{1}{T_{1/2.w}} + \frac{1}{T_{1/2.a}} C_a + \frac{1}{T_{1/2.N}} C_N, \qquad \text{Eq. 1}$$

With the relaxation times of water (w), agarose (a), and Ni-DTPA (N) and the concentrations C_a, C_N of agarose (%) and Ni-DTPA (mM), respectively. Additionally, the CT-value of the gels was modified by adding potassium chloride (KCl), which are expected not to change the relaxation times. Two exemplary MR contrasts (T_1=765ms, T_2=32ms and T_1= 1500ms, T_2=76ms at 1.5T) were produced containing seven different KCl concentrations, each. At a 1.5T MRI (Magnetom Symphony, Siemens Healthineers, Germany) a series of saturation recovery sequences and a multi-spin echo sequence with 32 equidistant echoes as implemented by the vendor were acquired to quantitatively measure T_1 and T_2 times, respectively. At a 0.35T MR-Linac (MRIdian Linac, Viewray, USA), the same type of measurements was performed for the T_1 quantification and a series of 8 double spin echo sequences for T_2 measurement.

[1] Tofts et al. 1993, doi: 10.1016/0730-725x(93)90420-i

Results

By adding KCl to the MRI contrast material positive CT-values up to 450 HU could be achieved without influencing T_1. As expected, T_1 decreases with higher field strength: (-53±28)ms and (-111±75)ms from 1.5 to 0.35T for the two samples, respectively. T_2 shows only a slight dependence on the KCl concentration, but, as expected, not significantly on the B-field. A linear fit characterizes the T_2 dependence as an offset of (0.04±0.01) and (0.15±0.05) l/(g ms)*[KCl] (95% confidence interval) for the two samples respectively as a function of the KCl concentration [KCl] in g/l.

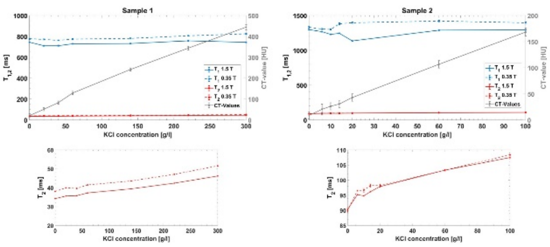

Figure 1: Dependence of T_1- and T_2- relaxation times and CT values on the KCl concentration at 0.35 and 1.5 T (top) with a zoom-in to the T_2 dependence (bottom) for two different phantom materials.

Conclusion

In this work, a method to produce phantom materials with adjustable T_1 and T_2 times was extended to simulate positive CT values up to 450HU by adding KCl. The dependence of the relaxation times on the KCl concentration and the field strength was investigated. This can be used for producing phantom materials with specified CT values and T_1 and T_2 relaxation times. Further measurements will focus on the generalization of the current results.